Final Report to
FDOT Structures Research Center
UF Project No. 00065162

August 2007

TESTING BRIDGE DECKS WITH NEAR-SURFACE MOUNTED FRP BARS EMBEDDED IN CEMENT BASED GROUT

Principal Investigator: H. R. (Trey) Hamilton III
Co-Principal Investigator: Antonis Michael

Graduate Research Assistant: Christina O'Neill

Project Manager: Marcus Ansley

Department of Civil & Coastal Engineering
College of Engineering
University of Florida
Gainesville, Florida 32611

Engineering and Industrial Experiment Station

DISCLAIMER

The opinions, findings, and conclusions expressed in this publication are those of the authors and not necessarily those of the State of Florida Department of Transportation.

ACKNOWLEDGMENTS

This research program was sponsored by the Florida department of transportation. The authors greatly acknowledge the contributions of the staff of the FDOT structures research center for their help in completing the experimental work. The contributions of Steve Eudy who set up and ran the data acquisition systems as well as the contributions of Frank Cobb, Paul Tighe, and David Allen who offered great assistance in specimen manufacturing and preparation of testing apparatus are greatly appreciated. The authors would also like to thank MMFX Steel Corporation of America for donating the MMFX reinforcing bars.

EXECUTIVE SUMMARY

Near-surface mounted (NSM) bars have been used for flexural strengthening of reinforced concrete members. The data available on this type of reinforcement technique are limited and typically, the bars or strips are embedded using an epoxy. Long term durability, abrasion resistance, and compatibility of the repair are important issues with this type of repair. One untested option for embedding the FRP bars into existing concrete is by using a Portland cement based grout. Laboratory specimens designed to represent bridge deck segments were strengthened using NSM bars embedded in a cement grout. Seven bridge deck segments were tested in flexure using three different types of NSM bars (GFRP, CFRP and MMFX bars) and two types of adhesive/filler materials (epoxy and cement based grout). The results indicate a significant improvement in the flexural capacity of all specimens strengthened using NSM bars. The epoxy adhered NSM specimens improved the most with an increase in the flexural capacity from 1.4 to 1.8 times the capacity of the control. The cement based grout adhered specimens had improved capacities of 1.3 to 1.4 times the capacity of the control. The failure mode of the epoxy specimens was concrete failure (concrete crushing or concrete shear failure) while the Portland cement grout specimens all had failure modes associated with bond (bar slippage or grout splitting) at the interface between the reinforcing bars and the Portland cement grout. The size of the cracks was reduced due to the NSM reinforcement. The crack sizes for the NSM reinforced specimens were up to 18 times smaller at failure compared to the cracks of the control bridge deck specimen.

TABLE OF CONTENTS

1 INTRODUCTION....1
2 SPECIMEN DESIGN....2
3 SPECIMEN MANUFACTURING....3
4 TEST SET-UP, INSTRUMENTATION AND TEST PROCEDURE....7
5 RESULTS AND DISCUSSION....8
6 THEORETICAL CAPACITY (ACI 440)....15
7 SUMMARY AND CONCLUSIONS....16
8 RECOMMENDATIONS....17
9 REFERENCES....18

1 Introduction

Near surface mounted (NSM) FRP bars have been used for flexural strengthening of reinforced concrete members. The data available on this type of reinforcement technique are limited. In all prior cases the FRP bars or strips were embedded in epoxy. No data are available on NSM FRP bars embedded in cement based grout. Since the effectiveness of the embedded reinforcement greatly depends on the bond between the FRP and the filler material and the bond between the filler material and the concrete, it is important to test this new approach before using it in the field. Testing could also determine failure modes for NSM FRP bars embedded in cement based grout.

The State of Florida is considering the use of NSM bars for the repair and strengthening of the Bow Channel Bridge located in the Florida Keys. The bridge is an old railroad concrete arch box bridge that has been modified to accommodate automobile traffic by extending the bridge deck on each side of the box. The new deck overhangs have generated negative bending stresses that have caused cracking on the top of the deck (see Figure 1). The proposed repairs call for the installation of transverse NSM bars in the deck surface to improve flexural capacity and control cracking. The current plans are to use epoxy to mount the NSM bars leaving epoxy exposed to weather and wear from traffic. Concerns about the long term durability of the epoxy due to exposure to Ultra Violet (UV) radiation prompted the decision to investigate the use of Portland cement based grouts to attach glue the reinforcement to the bridge deck. Cement based grouts have well known durability characteristics similar to concrete.

Literature on NSM FRP reinforcement for structural strengthening is limited. FRP bars are well suited for these types of applications because they are corrosion resistant and do not require a lot of cover for protection. In all cases found in the literature the NSM FRP bars or strips were installed using an epoxy. There are no data available relating to NSM bars or strips installed using Portland cement grouts.

El-Hacha and Rizkalla (2004) tested reinforced concrete T-beams in flexure using both carbon and glass NSM FRP bars and strips. They found that NSM carbon strips performed better than externally bonded carbon strips. The strength increase using the same CFRP strips as NSM reinforcement was approximately 4.8 times that obtained by externally bonding the carbon strips. The NSM CFRP bars were also very effective in improving the strength capacity of the beams although not as effective as the NSM CFRP strips. The failure mode for the NSM CFRP strips was rupture of the FRP while for the NSM carbon bars splitting of the epoxy cover.

Hassan and Rizkalla (2004) found that the efficiency of NSM bars is controlled primarily by the bond characteristics of the bars and the bond between the adhesive material and the concrete. They also indicated that rupture of the bar was unlikely regardless of the embedment length. Two different failure modes were observed: (1) splitting of the epoxy cover due to high tensile stresses at the FRP-epoxy interface (“epoxy split failure”), and (2) cracking of the concrete surrounding the epoxy adhesive (“concrete split failure”). Different embedment depths were also investigated and it was found that the most effective groove size for NSM bars was 1.5 times the diameter of the bar.

Nordin and Taljsten (2006) reinforced concrete beams with NSM CFRP prestressed bars. They also used an epoxy to embed the FRP bars. The prestressed NSM CFRP bars increased the load capacity of the beams by as much as 97%.

De Lorenzis and Nanni (2001(a)) used NSM bars to increase the shear capacity of concrete T-beams with and without steel stirrups. The bars were attached using an epoxy. The shear capacity of the beams with no steel stirrups was increased by up to 97% while the shear capacity of the beams with the steel stirrups was increased 35%.

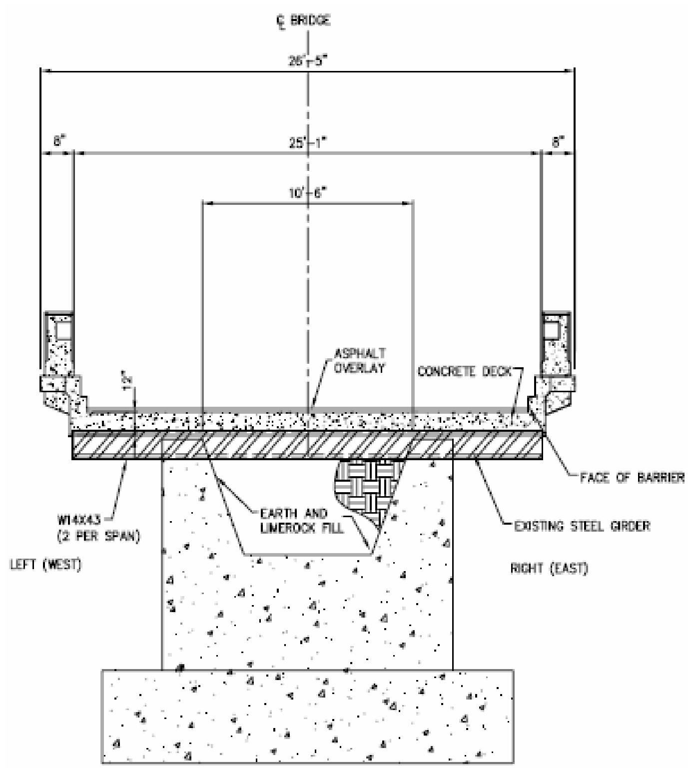

Figure 1 – Typical Section for Bow Channel Bridge (Adopted from Registe, Sliger Engineering).

2 Specimen Design

The 10 ft x 2 ft bridge deck specimen dimensions were sized to be easily handled in the laboratory. Although the bridge deck on the Bow Channel Bridge was 12 in. thick it was decided to use an 8 in. deck for the tests because it was easier to handle. However, no information on the location and amount of mild reinforcement was available and therefore the reinforcement ratio for the mild steel was unknown. The reinforcement ratios for the NSM reinforcement for the actual bridge deck were estimated based on the assumption of a 3 in. clear cover and #6 bars as mild steel reinforcement. The location of the NSM bars was selected to avoid overlap with the mild steel reinforcement. Carbon bars of 0.375 in. diameter were used to reinforce two of the deck segments. The size of glass FRP bars was selected to result in a comparable strength increase compared to carbon bar bridge segments. The same was done for the MMFX bar but a miscalculation resulted in the use of #5 bars instead of the #4 bars that would have comparable capacity to carbon and glass deck segments.

The two proposed repair options for the Bow Channel Bridge were #4 GFRP bars spaced at 12 in. and #6 MMFX bars spaced at 18 in both embedded in epoxy. The GFRP reinforcement ratio for the Bow Channel Bridge was 0.23% while for the bridge deck segments tested in the laboratory 0.37% which is significantly higher. The MMFX reinforcement ratio for the Bow

Channel Bridge was 0.46% almost the same as the bridge deck segments tested in the laboratory which had a ratio of 0.5%.

3 Specimen Manufacturing

Seven bridge deck segment specimens were constructed with the dimensions and mild steel reinforcement shown in Figure 2. Each segment was 10-ft long, 2-ft wide and 8-in. thick and reinforced with three ASTM A615, Grade 60, #6 mild steel bars. The segments were cast on the same day (see Figure 3) using a ready mixed concrete mixture with a specified 28-day strength of 4000 psi. The aggregate type was Florida limestone. Standard cylinders (6 x 12 in.) were cast to determine the concrete strength on test day.

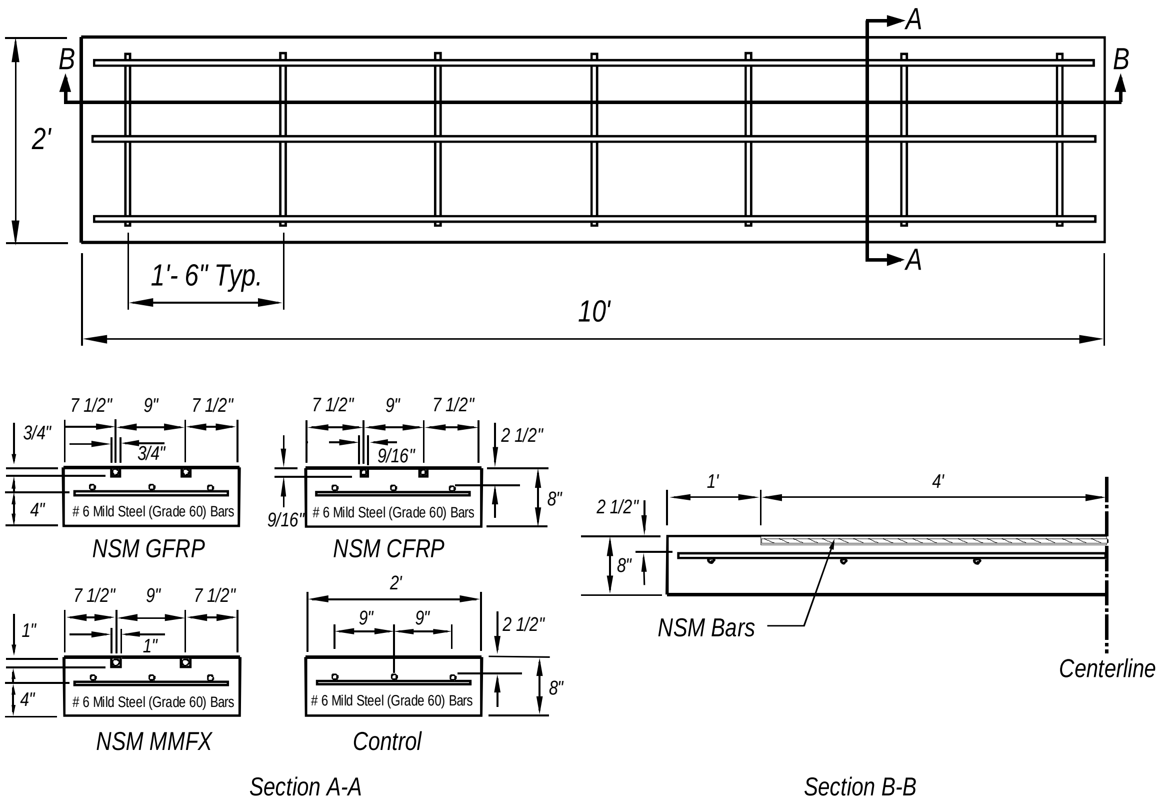

Figure 2 - Bridge Deck Segment Drawings.

The two different materials used to embed the NSM bars were an epoxy adhesive and a Portland cement based grout. The groves had a square cross-section as seen in Figure 4. All the details about the materials used and the sizes of reinforcement and grooves are listed in Table 1. Three different types of reinforcing bars were used: (a) glass FRP, (b) carbon FRP, and (c) MMFX steel.

Two grooves were cut in each specimen (centered lengthwise) with the exception of the control specimen (see Figure 5). Figure 2 shows the size and location of the grooves, which were 8 ft long and cut to 1.5 times the diameter of the NSM bar (Hassan and Rizkalla 2004; De Lorenzis and Nanni 2001(b)).

After the grooves were cut they were pressure washed to remove dust left from the saw cuts. Once dry, shots of compressed air eliminated any loose particles still present. The Portland cement grout was mixed and poured into the groove to approximately half the depth of the groove. The reinforcing bars were then placed into the groove, gently pressed into place and the groove was completely filled with grout (see Figure 6). The grout surface was then finished with a small trowel. The cement grout used was a non-shrink grout produced by Sika Inc. known with the trade name of SikaGrout 212. The same procedure was followed for the epoxy. The epoxy was dispensed into the groove using a grout bag (see Figure 7). The epoxy used was also a Sika Inc. product known as SikaDur 30. SikaDur 30 is a two part epoxy with 100% solids that has a paste consistency.

Figure 3 – Casting of Bridge Deck Segments.

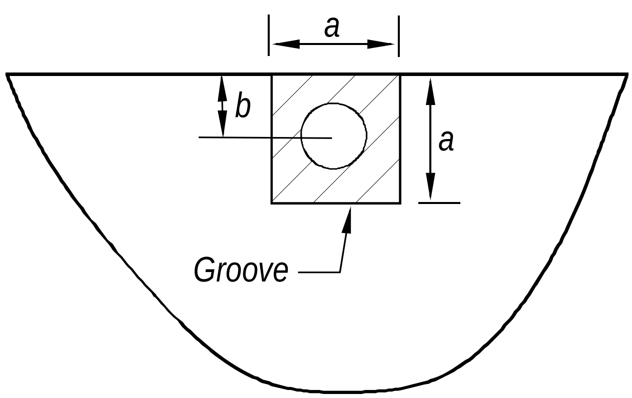

Figure 4 – Groove Detail.

Table 1 – NSM Specimen Details.

Specimen	# of NSM Bars	NSM Bar Size	Groove Size		Type of Adhesive/Filler
			a (in.)	b (in.)	
Control	N/A	N/A	N/A	N/A	N/A
GLEP	2	# 4	3/4	3/8	Epoxy
GLCE	2	# 4	3/4	3/8	Cement Based
CAEP	2	# 3	9/16	9/32	Epoxy
CACE	2	# 3	9/16	9/32	Cement Based
MMFXEP	2	# 5	1	0.5	Epoxy
MMFXCE	2	# 5	1	0.5	Cement Based

GL = Glass bar, CA = Carbon bar, EP = Epoxy, CE = Cement grout

Figure 5 - Groove Cutting.

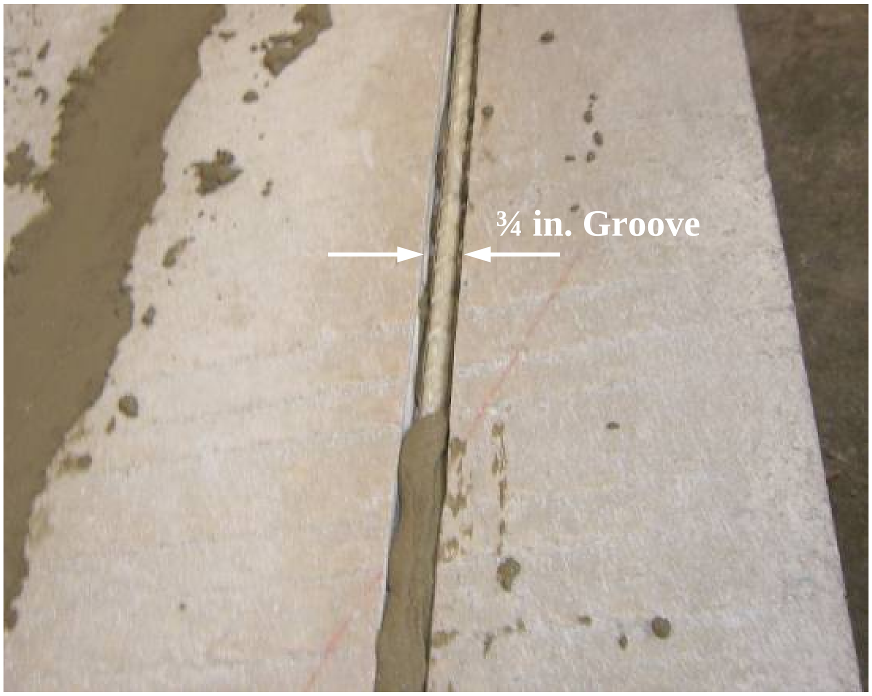

Figure 6 – NSM Bar Installation Using Cement Grout.


Figure 7 – NSM Bar Installation Using Epoxy.

The following notation was used to identify variables in each specimen:

- GL = Glass FRP reinforcing bar
- CA = Carbon FRP reinforcing bar
- MMFX = Microcomposite Multistructural Formable Steel
- EP = Epoxy
- CE = Cement grout

For example, the specimen labeled GLEP had glass FRP bars embedded using epoxy.

4 Test Set-Up, Instrumentation and Test Procedure

The bridge deck segments were tested under a four point loading configuration. Figure 9 shows that the segments were loaded such that the tension face was oriented upward to allow cracking to be visible during loading. Eleven displacement gages (LVDTs) were used to record the displacement at various locations. Two strain gages, one longitudinal and one transverse, were installed in the compression zone, at mid-span. The actual test set-up for the control specimen can be seen in Figure 10. A loading rate of approximately 0.002 in./sec was used to load the specimens. This loading rate was selected to ensure a static loading and avoid a strain rate which would alter the strength characteristics of the concrete. The compressive strain rate in the concrete was monitored during the test using the data recorded by the longitudinal strain gage. The loading rate resulted in a strain rate of 3 με/sec or less. According to data available in the literature, for concrete loaded in compression, a strain rate of 3 με/sec or less has no significant (less than 10%) effect on the strength of concrete (Ross et al. 1996; Ross, Tedesco and Kuennen 1995). Therefore, the strain rate used in the testing of the bridge deck specimens did not have an effect on concrete strength.

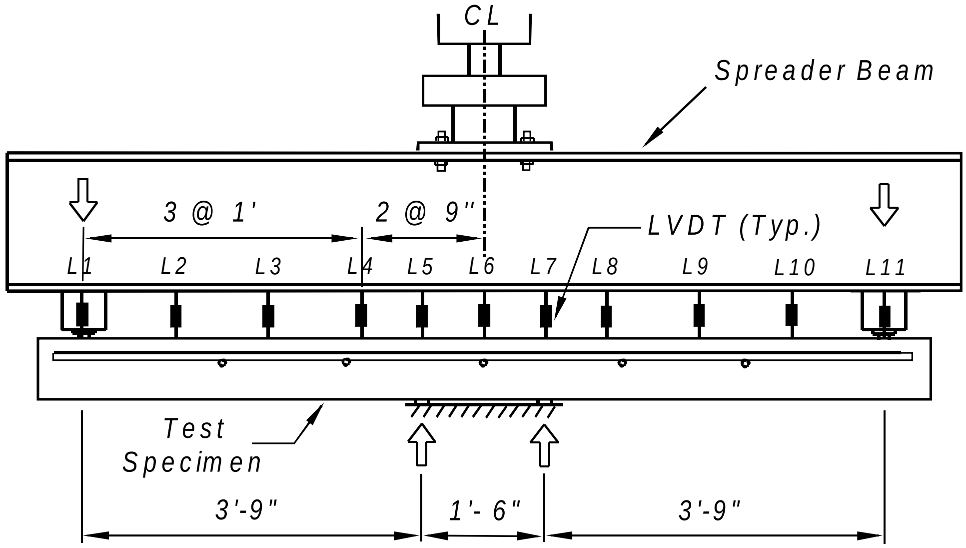

Figure 9 – Test Set-Up and Instrumentation.

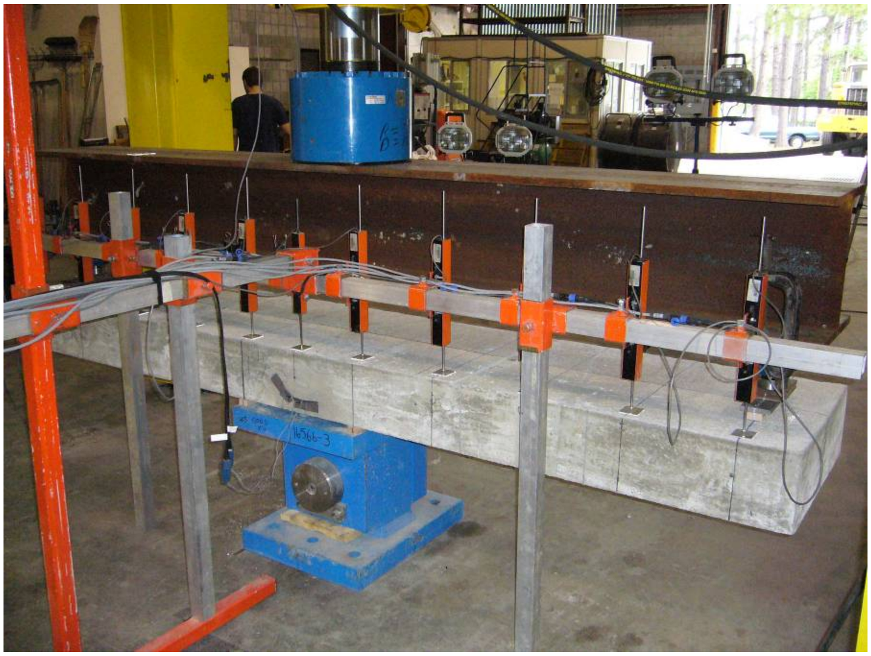

Figure 10 – Test Set-Up for Control Specimen.

5 Results and Discussion

The load-displacement curves of the bridge deck specimen are shown in Figures 11 trough 13. The load and displacement values are the average values of the cantilever ends of the bridge deck specimens. The control specimen failed due to concrete crushing after the mild steel reinforcement yielded. All specimens reinforced with NSM bars had a significant increase in stiffness and strength. The specimens with the epoxy adhesive had higher strength increases than the specimens with the cement based grout. Specimen CAEP had a strength increase of 55%, specimen GLEP 40% and specimen MMFXEP 82% compared to the control specimen. Specimen CACE had strength 25% higher than the control specimen while specimens GLCE and MMFXCE had a strength increase of 27% and 37% respectively. The type of adhesive material had a significant effect on the strength increase with the epoxy providing a higher increase than the Portland cement grout.

The observed failure modes for all the specimens are listed in Table 2. In general, the specimens with the Portland cement grout had a failure mode associated with bond failure. For the specimens with cement grout and the FRP bars (CACE and GLCE) the failure was due primarily to slippage of the FRP bars (see Figure 14). However, it was also observed that in a few spots the cement grout split. The split was not nearly as extensive as in the case of the MMMFXCE specimen where failure was due to splitting of the Portland cement based grout (see Figure 15). The rest of the specimens, with the epoxy adhesive, had flexural failure modes (concrete crushing after yielding of the mild steel [see Figure 16(a)]) or in the case of specimen MMFXEP a shear failure mode due to over reinforcing (see Figure 16(b)). Rupture of the NSM bars did not occur during the tests.

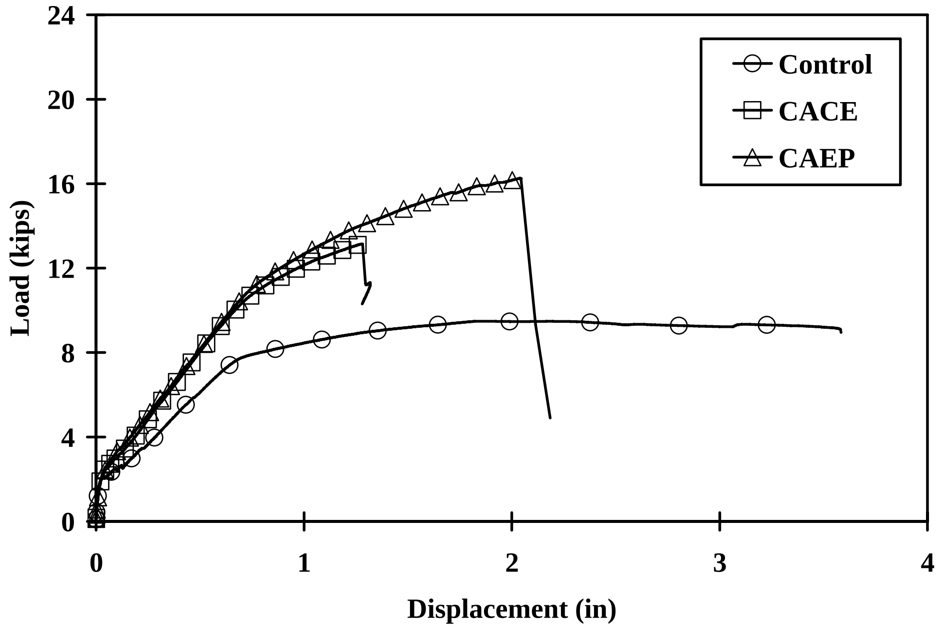

Figure 11 – Load-Displacement Curves for Control, CACE and CAEP Specimens.

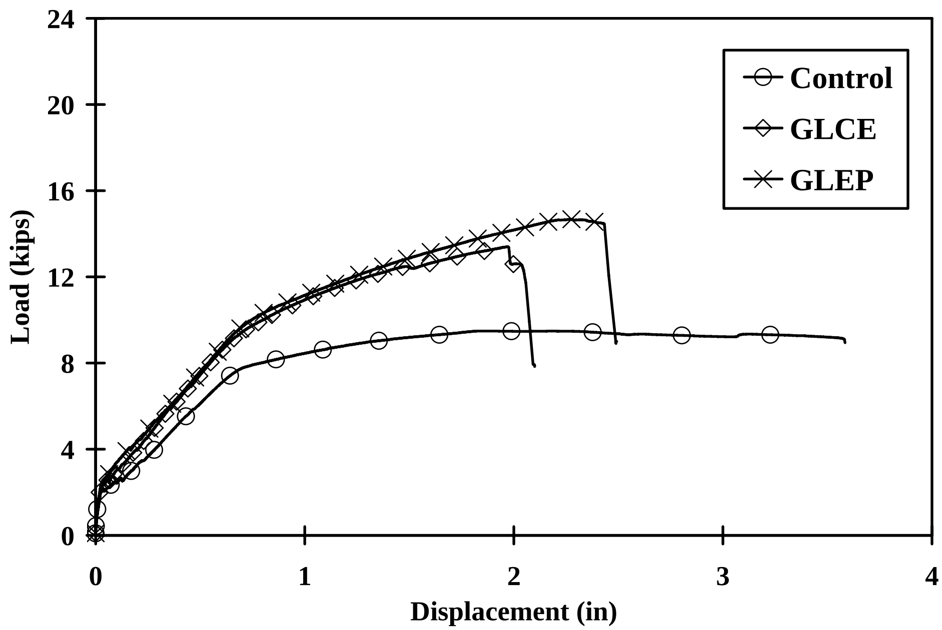

Figure 12 – Load-Displacement Curves for Control, GLCE and GLEP Specimens.

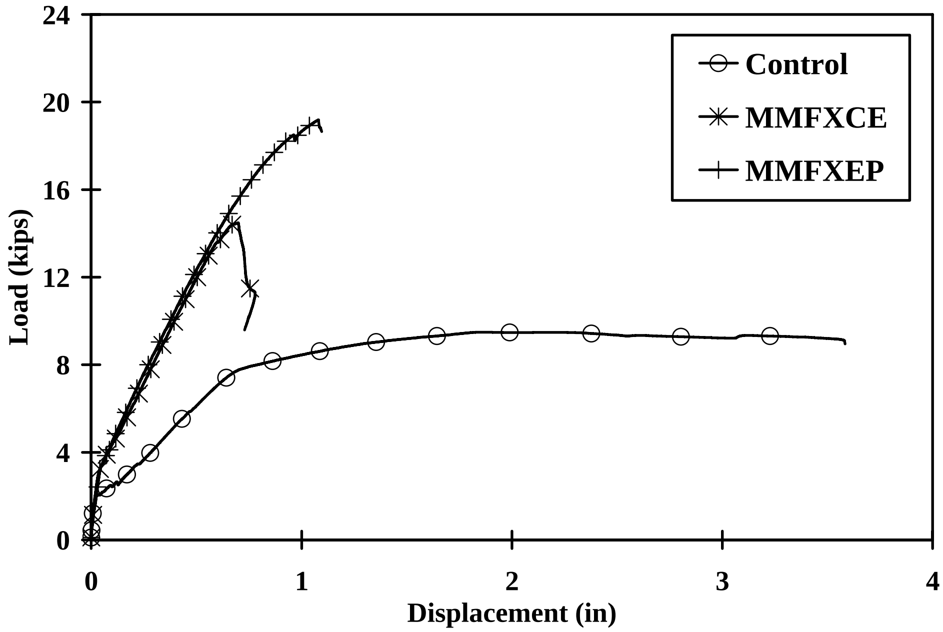

Figure 13 – Load-Displacement Curves for Control, MMFXCE and MMFXEP Specimens.

Table 2 – NSM Specimen Details.

Specimen	Exp. Load (kips)	ACI Load (kips)	Exp./ ACI 440	Failure Mode
Control	21	16.4	1.28	Concrete crushing
GLEP	29.5	28.3	1.04	Concrete crushing
GLCE	26.7	28.3	0.94	NSM bar slip
CAEP	32.5	31.4	1.04	Concrete crushing
CACE	26.2	31.4	0.83	NSM bar slip
MMFXEP	38.3	37.1	1.03	Shear at east end
MMFXCE	28.8	37.1	0.78	Grout Splitting

The ductility of the NSM reinforced specimens was lower than the ductility of the control specimen as seen in the load-displacement curves (Figures 11 through 13). However, the bridge deck specimens with flexural failure modes demonstrated significant ductility compared to the specimens with bond or shear failure modes. The displacement ductility factor ($\mu_\Delta = \Delta_u / \Delta_y$) for the control specimen was approximately 4.8. The ductility factors for specimens CAEP and GLEP were 2.7 and 3.2, respectively. Specimen GLCE had a ductility factor of 2.8 and specimen CACE value was 1.6. This indicates that even though specimen GLCE failed due to bond the glass FRP bar developed a better bond with the cement grout than the carbon bar. The specimens with the microcomposite steel had low ductility factors because the bar was not fully developed due to slip. Specimen MMFXEP failed in shear resulting in a ductility factor of 1.4. Specimen MMFXCE had a ductility factor of 1.1. The highest ductility from the NSM reinforced specimens was exhibited by specimen GLEP, which demonstrated 67% of the ductility of the control specimen. The lowest ductility factor was by specimen MMFXCE which had a value of 23% of the control specimen.

(a) (b)

Figure 14 – FRP Bar Slippage for Specimen: (a) CACE and (b) GLCE.

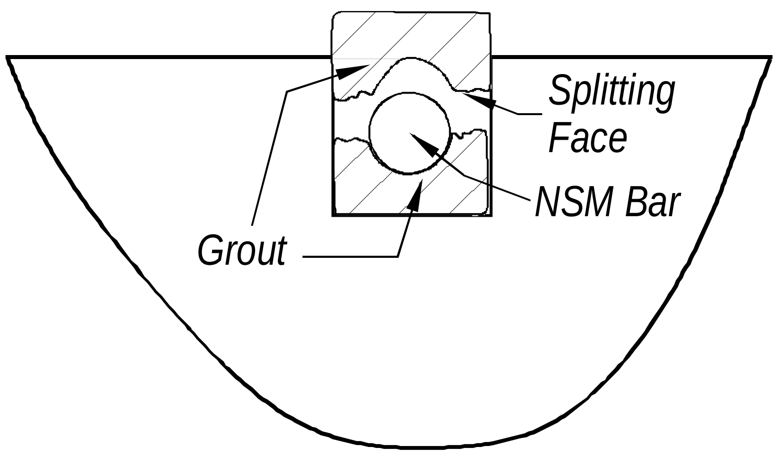

Figure 15 – Splitting of Cement Based Grout.

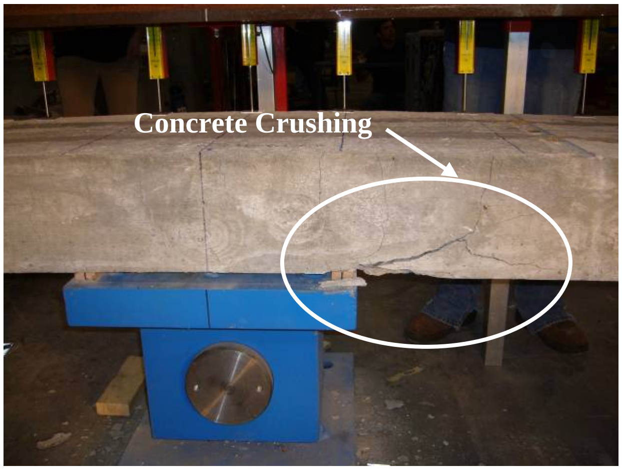

(a)

(b)

Figure 16 – Failure Modes for Epoxy Specimens: (a) Concrete Crushing and (b) Shear.

As it was mentioned in a previous section of the report, the NSM reinforcement ratio for the MMFX reinforcement was same as the reinforcement ratio for the Bow Channel Bridge proposed repair method using the MMFX steel as NSM reinforcement. This reinforcement ratio, if selected, is likely to result in similar behavior in the actual bridge. Although specimen MMFXEP had the highest capacity of all specimens it also had the lowest ductility. Therefore, it is reasonable to assume that if the specific repair option is adapted the actual bridge deck will loose much of its ductility much like specimen MMFXEP (see Figure 13). It could also lead to a change in the failure mode of the deck similar to the case of specimen MMFXEP where the mode changed from a flexural mode (control specimen) to a shear mode (MMFXEP). The shear mode is a non-ductile failure mode and it should be avoided if possible.

The same observations as in the case of the load-displacement curves were made for the moment-curvature (M-Φ) curves (see Figures 17 through 19). The M-Φ curves seen in Figures 17 through 19 were developed using the displacement profiles for each specimen at different loads. For each different load the displacement profile was plotted using the readings from the LVDTs and the equation for each profile was derived by fitting a curve through the experimental displacement points. Then, by taking the second derivative of the displacement equation the curvature was calculated at a specific section of the bridge deck segment. In this case the curvature was calculated at the centerline of each bridge deck segment.

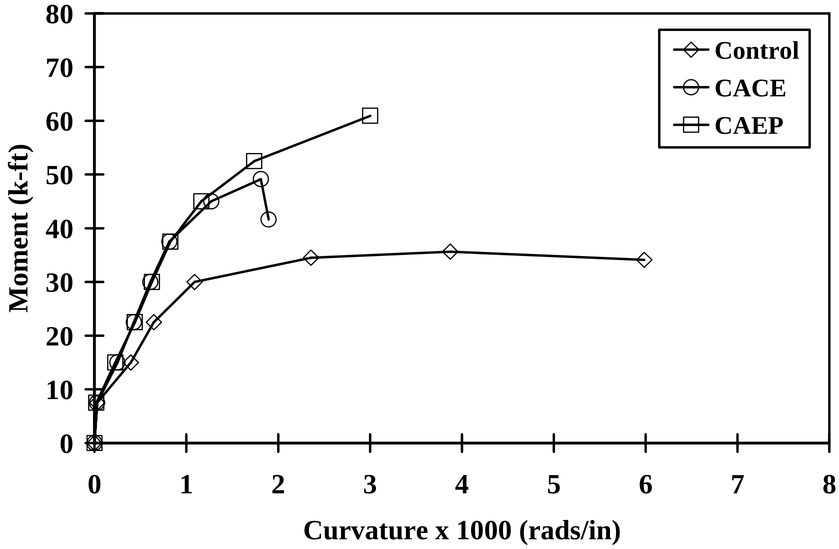

Figure 17 – M-Φ Curves for Control, CACE and CAEP Specimens.

Using the M-Φ curves the curvature ductility factors ($\mu_{\Phi} = \Phi_u / \Phi_y$) were calculated. The control specimen had a curvature ductility factor of 5.6. The ductility factors for specimens CAEP and GLEP were 2.9 and 3.8, respectively. Specimen GLCE had a ductility factor of 3 and specimen CACE value was 1.8. Specimen MMFXEP had a curvature ductility factor of 1.4 and specimen MMFXCE a ductility factor of 1.1. The highest ductility from the NSM reinforced specimens was exhibited by specimen GLEP, which demonstrated 68% of the ductility of the control specimen. The lowest ductility factor was by specimen MMFXCE which had a value of 20% of the control specimen. Although the values of the displacement and curvature ductility factors are different the relative ductility of the specimens compared to the control specimen is approximately the same irrespectively of the ductility factor used.

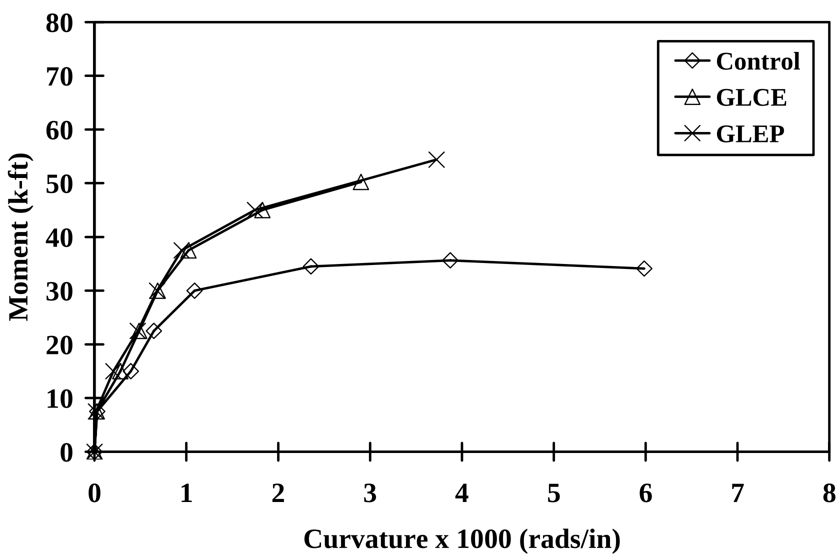

Figure 18 – M-Φ Curves for Control, GLCE and GLEP Specimens.

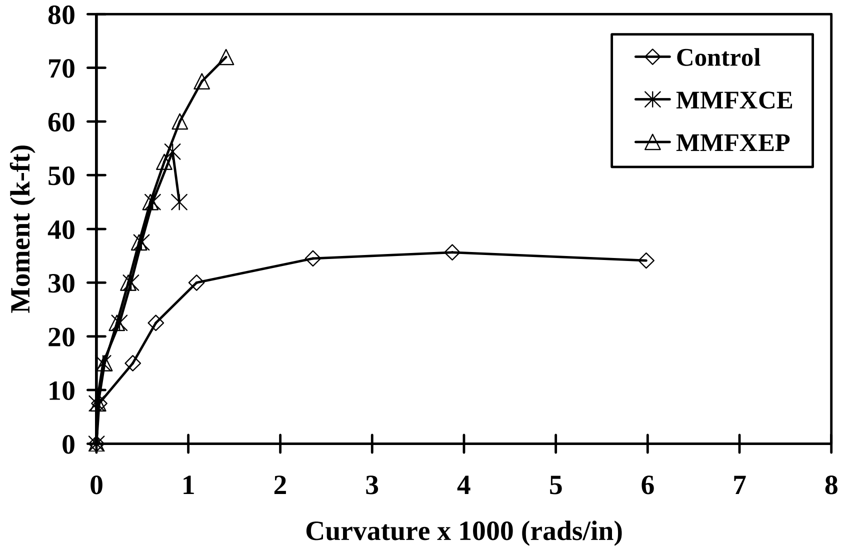

Figure 19 – M-Φ Curves for Control, MMFXCE and MMFXEP Specimens.

The cracking patterns in the mid-span region between the two supports of the various bridge deck specimens were very similar. The flexural cracks were evenly spaced and formed at approximately the same locations for all bridge deck specimens. The difference was the size of the cracks. Although the crack sizes were not measured during the tests it was visibly apparent that the crack sizes of the bridge deck segments reinforced with the NSM bars were smaller in size than the cracks of the control specimen. The crack sizes were measured after testing and for the control specimen the cracks were approximately 0.19 in. wide while the cracks for the NSM reinforced specimens varied from approximately 0.01 in. to 0.05 in. The measured crack widths for the bridge deck segments are listed in Table 3.

Table 3 – Crack Widths.

Specimen	Crack	Crack Size (in.)	Aver. Crack Size (in.)
Control	1	0.19	0.19
	2	0.19	
	3	0.19	
GLEP	1	0.04	0.04
	2	0.04	
GLCE	1	0.05	0.05
	2	0.04	
	3	0.05	
CAEP	1	0.03	0.04
	2	0.05	
	3	0.04	
CACE	1	0.04	0.05
	2	0.04	
	3	0.06	
MMFXEP	1	0.01	0.01
	2	0.01	
	3	0.01	
MMFXCE	1	0.03	0.02
	2	0.01	

6 Theoretical Capacity (ACI 440)

Using the guidelines provided by ACI Committee 440 (ACI Committee 440 2002) the theoretical and experimental capacities for the bridge deck specimens were calculated and are compared in Table 2. The concrete strength was determined through cylinder tests (average *f'c* = 5680 psi). The results from the cylinder tests are listed in Table 4. The properties of the NSM bars were obtained from the manufacturer (see Table 5 for NSM bar properties).

The calculated capacities for the bridge deck specimens with the epoxy adhesive were approximately 4% lower than the experimental ones. The theoretical capacities of the bridge deck specimens with the Portland cement grout were higher than the experimental ones by as much as 22%. This was due to the bond failure modes associated with these specimens. ACI 440.2R-02 addresses bond issues with a bond reduction coefficient for externally bonded FRP reinforcement. It would seem logical to have a similar coefficient for NSM reinforcement embedded with Portland cement grout. In order to achieve this, bond characteristics between Portland cement grouts and NSM reinforcing bars need to be investigated.

Table 4 – Cylinder Test Data.

Cylinder	Strength (psi)	Aver. Strength (psi)
1	5581	5684
2	5653	
3	5573	
4	5932	
5	5675	
6	5721	
7	5658	
8	5890	
9	5658	
10	5710	
11	5615	
12	5765	
13	5470	

Table 5 – NSM Bar Properties.

Bar Type	Size	Area (in^2)	Yield Strength (ksi)	Ultimate Strength (ksi)	MOE (ksi)
Carbon	#3	0.101	N/A	300	18000
Glass	#4	0.225	N/A	100	5900
MMFX	#5	0.31	100	185	29000

7 Summary and Conclusions

Based on the data and observation from the flexural tests conducted on the bridge deck segments the following conclusions can be drawn:

- The epoxy adhesive was more effective in increasing the capacity of the bridge deck specimens. The capacity of the NSM reinforced specimens was up to 1.82 times higher than the capacity of the control specimen. This was due to the superior adhesion provided by the epoxy compared to the Portland cement grout.
- The Portland cement grout was not as effective as the epoxy adhesive. However, the capacity of the bridge deck specimens with the cement grout was increased by up to 37% compared to the control specimen.
- The Bow Channel Bridge repair option with the MMFX steel used as NSM reinforcement should be revaluated to make sure that it will not result in a non-ductile failure mode. The fact that the NSM reinforcement ration is the same as the ratio used in the laboratory specimens with the same reinforcement is a strong indication that the failure mode observed in the laboratory will be the same if this particular option is adopted. Therefore, caution should be exercised and the option revaluated to avoid such failure mode.
- Crack sizes were significantly reduced with the use of the NSM reinforcement. The largest cracks measured in the NSM reinforced bridge deck specimens were approximately 3.5 times smaller than the cracks measured for the control bridge deck specimen.

8 Recommendations

The groove size for the specimens with the Portland cement grout was based on recommendations from tests conducted on specimens with epoxy adhesive. It is probable that Portland cement grout would be more effective with deeper and possibly wider grooves. Therefore, the influence of the groove size to the effectiveness of the Portland cement grout needs to be investigated to determine the optimal size for this type of material.

Wetting the grooves is recommended before placing the grout to facilitate better bond and to avoid the concrete extracting moisture from the cement based grout which could result in voids due to flash setting of the grout.

It is evident that the epoxy outperformed the Portland cement based grout but the issue of long term durability of the epoxy when exposed to UV radiation still remains. It is well accepted that UV radiation leads to degradation of the epoxy (Malvar 1998; Hamilton and Dolan 2000; Pantelides et al. 2004) and the use of additives or coatings is required. However, in the case of the Bow Channel Bridge a UV protective coating will be exposed to traffic and will be eroded. Pantelides et al. reported that the protective coats are also vulnerable to UV radiation and that puts into question their effectiveness even if they are not eroded by an external factor such as traffic. Pantelides et al. reported that the UV protective coating deteriorated within 2 to 3 years and the epoxy under it showed signs of degradation. The problem will be more serious in the case of the Bow Channel Bridge because of the location of the bridge and the all year severe UV exposure the bridge experiences in the Florida Keys. One solution would be to make the grooves deeper and partly filled them with the epoxy leaving a top layer to be filled with a Portland cement based grout. The top layer can be ¾ to 1 in. which will require the groove to be cut deeper by the same amount. Another option will be to again make the groove deeper but only use the epoxy at the two ends of the groove to provide enough anchorage to fully develop the bars and then fill the rest of the space with the Portland cement based grout. The Portland cement grout has properties similar to concrete which are well known and it is expected to perform the function of the wearing surface like the surrounding concrete bridge deck.

9 References

ACI Committee 440, 2002, “Design and Construction of Externally Bonded FRP Systems for Strengthening Concrete Structures (440.2R-02),” American Concrete Institute, Farmington Hills, Michigan, 45 pp.

De Lorenzis, L., and Nanni, A., 2001(a), “Shear Strengthening of Reinforced Concrete Beams with Near-Surface Mounted Fiber-Reinforced Polymer Rods,” ACI Structural Journal, Vol. 98, No 1, pp. 60-68.

De Lorenzis, L., and Nanni, A., 2001(b), “Characterization of FRP Rods as Near-Surface Mounted Reinforcement,” Journal of Composites for Construction, Vol. 5, No 2, pp. 114-121.

El-Hacha, R., and Rizkalla, S. H., 2004, “Near-Surface-Mounted Fiber-Reinforced Polymer Reinforcements for Flexural Strengthening of Concrete Structures,” ACI Structural Journal, Vol. 101, No 5, pp. 717-726.

Hamilton III, H. R., and Dolan, C. W., 2000, “Durability of FRP Reinforcements for Concrete,” Progress in Structural Engineering and Materials, Vol. 2, pp. 139-145.

Hassan, T. K., and Rizkalla, S. H., 2004, “Bond Mechanism of Near-Surface-Mounted Fiber-Reinforced Polymer Bars for Flexural Strengthening of Concrete Structures,” ACI Structural Journal, Vol. 101, No 6, pp. 830-839.

Malvar, L. J., 1998, “Durability of Composites in Reinforced Concrete,” CDCC’98 - First International Conference on Durability of Composites for Construction, Sherbrooke (Québec), Canada, August 1998.

Nordin, H., and Täljsten, B., 2006, “Concrete Beams Strengthened with Prestressed Near Surface Mounted CFRP,” Journal of Composites for Construction, Vol. 101, No 6, pp. 830-839.

Pantelides, C.P., Reay, J., Reaveley, L.D., and Ring, T.A., 2004, “Long Term Durability of Carbon FRP Composites Applied to RC Bridges: State Street Bridge on Interstate 80 – Final Report 1st Phase.” Report No. CVEEN-04/1, Department of Civil and Environmental Engineering, University of Utah, Salt Lake City, Utah, March 2004, 83 pages.

Ross, C. A., Jerome, D. M., Tedesco, J. W., and Hughes, M. L., 1996, “Moisture and Strain Rate Effects on Concrete Strength,” ACI Materials Journal, Vol. 93, No 3, pp. 293-300.

Ross, C. A., Tedesco, J. W., and Kuennen, S. T., 1995, “Effects of Strain Rate on Concrete Strength,” ACI Materials Journal, Vol. 92, No 1, pp. 1-11.